2nd Mercosur Congress on Chemical Engineering
4th Mercosur Congress on Process Systems Engineering

SIMPLIFIED MODELS FOR SINGLE-SCREW EXTRUSION APPLICATIONS

L. A. Vignol[1], N. S. Cardozo[1*], A. R. Secchi[1], F. Angiolini[2], M. D. Pizzol[2],
[1]Departamento de Engenharia Química - Universidade Federal do Rio Grande do Sul
[2]Desenvolvimento e Tecnologia - Innova S/A

Abstract. In this work, simplified models for the prediction of mass flow rate and pressure at the exit of single-screw extruders as functions of material properties and extruder operating conditions are presented. These models were developed using experimental data and predictions of a commercial extrusion simulator, and can be used for fast decision making related to the extruder operating conditions during resin changes. Experimental values of mass flow rate and pressure at the exit of a 45 mm single-screw extruder were measured while processing polypropylene (PP) and polystyrene (PS). These tests were performed by varying screw speed from 70 up to 100 rpm. Then, a first set of simulations was carried out by using Flow 2000 computational package (Compuplast, Inc.) in order to fit the simulator predictions to the PP and PS extrusion experimental data, through the estimation of the barrel-polymer friction coefficients. Afterwards, a second set of simulations was carried out according to a $2^{(20-14)}$ fractional factorial design of experiments (DOE), using material properties (rheological and thermal) and extruder processing conditions (screw speed and barrel temperature profile) as factors for investigation. The Flow 2000 predictions of mass flow rate and pressure at the exit of the extruder at the DOE points were used for fitting the parameters of the simplified models. These simplified models were developed by combining linear terms with some well-known nonlinear relations, such as the dependence of the mass flow rate on the viscosity. Good agreement between experimental and predicted values was achieved when the simplified models were applied.

Keywords: Extrusion Simulation, Polystyrene Extrusion, Polypropylene Extrusion.

1. Introduction

Extrusion is a technology widely used in the plastic, pharmaceutical and food industries. In the plastic industry, extrusion is a process applied in the continuous production of polymer parts, such as pipes, tubes, films, and sheets. It involves several complex phenomena, such as solids conveying, heat transfer, phase change, and flow of non-Newtonian fluids. Rauwendaal (1986) presents a detailed description of the functional zones of single and twin-screw extruders (solids conveying, melting and melt conveying). Due to its practical importance, great attention has been paid to the modelling of the physical phenomena involved in single-screw extrusion during the last decades. Cunha (2000) presents a good review about single-screw extrusion modelling and simulation. The mathematical description of the flow of polymer into single-screw extruders has allowed the development of 2D and 3D simulation software for screw project and fault diagnosis purposes. In addition, great efforts have been made to develop optimization schemes for determining the operating conditions or screw geometry that produce a desired performance.

Despite the remarkable progress achieved in the development of simulation programs, the use of these computational packages in polymer extrusion applications is still limited. Probably, this situation is a result of the fact that such packages require high investment and specialized human resources for carrying out a reliable analysis of the process. A possible alternative to these complex simulation tools can be achieved by means of the

* To whom all correspondence should be addressed.
Address: Dept. de Engenharia Química, UFRGS - Campus Centro, s/n, CEP: 90040-040, Porto Alegre – Brazil
E-mail: nilo@enq.ufrgs.br

development of semi-empirical models for polymer extrusion. Thus, a compromise among accuracy, physical clearness, low computational time, low cost, and simplicity of use can be obtained.

The main goal of this work is to present simplified models for the prediction of mass flow rate and pressure at the exit of the extruder as functions of material properties and extruder operating conditions. These models were developed using experimental data and predictions of a commercial extrusion simulator and can be used for fast decision making related to the extruder operating conditions during resin changes.

2. Materials and methods

2.1. Materials

An isotactic polypropylene (PP), supplied by Petroquimica Cuyo S/A, and a general purpose polystyrene (PS), supplied by Petrobras Energía S/A, were used as sample materials. Table 1 summarizes some thermal and physical properties of these materials.

Table 1. Thermal and physical properties of the materials.

Property	PP	PS
Melt flow rate (MFR), g/10 min	2.45	4.21
Density in solid state (ρ_s), kg/m^3	899[1]	1043[1]
Specific heat in solid state (Cp_s), J/kg.°C	1700[2]	1218[3]
Thermal conductivity in solid state (k_s), W/m.°C	0.284[4]	0.123[5]
Melting temperature (T_m), °C	163[6]	155[3]
Melting enthalpy (ΔH_f), J/kg	107930[6]	0[3]
Density in molten state (ρ_m), kg/m^3	792[1]	998[1]
Specific heat in molten state (Cp_m), J/kg.°C	2100[2]	1923[3]
Thermal conductivity in molten state (k_m), W/m.°C	0.156[4]	0.159[5]
Bulk density (ρ_b), kg/m^3	555	622
Barrel-polymer friction coefficient (f_b)	0.450[2]	0.450[2]
Screw-polymer friction coefficient (f_s)	0.200[2]	0.200[2]

1 - MC Base, 2002; 2 - Flow 2000, 2002; 3 - Han et al., 1996; 4 - Zhang et al., 2002; 5 - Moore, 1989; 6 - Wolf and Grave, 2002.

Since polystyrene is an amorphous polymer, not presenting a true melting temperature, the "T_m" of the PS was calculated as T_g + 55°C, according to the approach of Han et al. (1996). According to the manual of the commercial software, PP and PS present same values for f_b and f_c, however, this seems to be improbable. Thus, the friction coefficients indicated by manual of the software were used only as an initial guess in the simulations.

2.2. Rheometry

The rheological characterization of the samples of PS and PP was carried out in a rotational rheometer ARES (Rheometric Scientific). Frequency sweep tests were performed in order to obtain data of complex viscosity (η^*) at angular frequencies (ω) from 0.1 up to 500 rad/s at temperatures of 190°C, 210°C, and 230°C for each sample. The modified Andrade-Eyring model (Flow 2000, 2002) and the Carreau-Yasuda model (Menges and Osswald, 1996) were used to express the viscosity dependence on temperature and shear rate, respectively, resulting in Eq.(1).

$$\eta(\dot{\gamma},T)=\frac{\eta_0 e^{-b(T-T_{ref})}}{[1+(\lambda e^{-b(T-T_{ref})}\dot{\gamma})^a]^{\frac{1-n}{a}}} \quad (1)$$

where $\eta(\dot{\gamma},T)$ is the shear viscosity; η_0, λ, a, n and b are the parameters whose values must be estimated at arbitrary reference temperature, T_{ref}.

2.3. Extrusion

Extrusion tests were performed in a 45 mm single-screw extruder with L/D of 25. Table 2 presents the main characteristics of the extruder screw used in this study.

Table 2. Characteristics of the screw.

Screw diameter (mm)	45
Screw length (mm)	1118.0
Feed section length (mm)	170.0
First compression section length (mm)	420.0
Second compression section length (mm)	80.0
Metering section length (mm)	448.0
Feed section depth (mm)	8.5
First compression section depth (mm)	4.9
Second compression section depth (mm)	2.1
Screw pitch (mm)	45
Flight width (mm)	5.6

The extruder was divided in five zones: a feed zone, without temperature control, and four heating zones, with independent control of the external surface temperature of the barrel (T_e) provide by PID controllers. Each heating zone was also equipped with additional P and T sensors to monitor the value of these variables near the internal surface of the extruder barrel. Table 3 shows barrel heating zones and positions of the sensors along the screw axis:

Table 3. Barrel heating zones and sensors positions along the screw axis.

Heating zone	*Initial position (mm)*	*Final position (mm)*	*Position of the external sensor (mm)*	*Position of the internal sensor (mm)*
Zone 1	154	394	274	310
Zone 2	394	634	514	600
Zone 3	634	864	749	773
Zone 4	864	1154	1009	1154

As shown in Table3, the fourth internal sensor is located at exit of the extruder (1154 mm). Actually, this sensor is positioned into a metallic plate located between the exit of the extruder and the entrance of the die. Consequently, the temperature values indicated by this sensor (T_{exit}) are not important for the development of the simplified models, since these values do not represent the behavior of the material neither into the screw channels nor into the die channels. Contrarily, the pressure values indicated by the sensor at this position are very important, since they correspond to the pressure at the exit of the extruder, P_{exit}.

The extrusion tests were carried out at constant screw speed (*N*), ranging from 70 up to 100 rpm. For each screw speed, the tests were repeated three times and the results were averaged. The temperature profiles used in the tests are shown in Table 4, where T_{set} represents the temperature set in a given heating zone.

Table 4. Barrel temperatures for PP and PS extrusion tests.

Barrel Heating Zone	T_{set} for PP (ºC)	T_{set} for PS (ºC)
Zone 1	200.0	190.0
Zone 2	200.0	195.0
Zone 3	200.0	200.0
Zone 4	200.0	200.0

A die plate with circular holes was used to produce molten strands of polymer. Extruded material was collected at intervals of 1 min and weighed in order determine the mass flow rate values. In all tests, the die temperature (T_{die}) was maintained at 200°C.

2.4. Simulation

The Flow 2000 software (Compuplast Inc.) was used for performing the extrusion simulations. This software uses Rauwendaal (1986) and Tadmor (1970) models for describing solid conveying and melting processes, respectively. In every cross-section, the variables are calculated by using 1D FEM and in the down-channel direction by using 2D FDM. The input data for the Flow 2000 were the rheological, thermal and physicals properties of the materials and the geometric characteristics and operating conditions of the extruder.

3. Results and Discussion

3.1. Rheology

The data of complex viscosity obtained by rotational rheometry were fitted to the rheological model, Eq. (1), using 190°C as reference temperature. The estimated values of the rheological parameters are shown in Table 5, and Fig. 1 shows a comparison between experimental and predicted complex viscosity curves of the PP and PS samples.

Table 5. Rheological parameters of the polymers at 190°C.

Parameter	PP	PS
η_0 (Pa.s)	17710	26186
n	0.15	0.21
a	0.38	0.53
λ (s)	0.21	0.61
b ($°C^{-1}$)	0.037	0.059

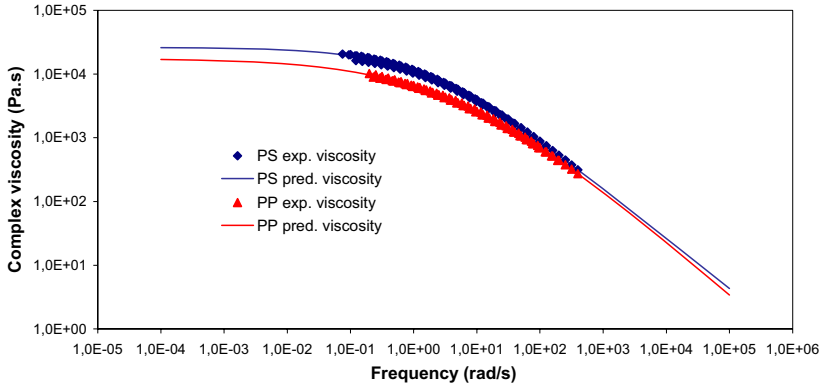

Fig. 1. Comparison between experimental and predicted values of the complex viscosity of the polymers at 190°.

Figure 1 shows that good agreement between experimental and predicted curves of complex viscosity was achieved for both PP and PS, allowing the use of the rheological parameters as input data for simulations.

3.2. Extrusion

It was necessary to collect data for $\dot{m}$ and P_{exit} in order to verify the predictions of the commercial simulator. Table 6 and 7 shows the values of mass flow rate and pressure obtained in the extrusion of the polypropylene and polystyrene samples, respectively. The values measured by the internal and external temperature sensors and the pressure sensor in each zone, and the screw speed are also presented in these tables.

Table 6. Results of the polypropylene extrusion.

	T_{set1}=200°C T_{e1}=206°C		T_{set2}=200°C T_{e2}=205°C		T_{set3}=200°C T_{e3}=204°C		T_{set4}=200°C T_{e4}=206°C			
N *(rpm)*	P_{i1} *(MPa)*	T_{i1} *(°C)*	P_{i2} *(MPa)*	T_{i2} *(°C)*	P_{i3} *(MPa)*	T_{i3} *(°C)*	P_{exit} *(MPa)*	T_{exit} *(°C)*	T_{die} *(°C)*	$\dot{m}_E$ *(kg/h)*
70.0	35.0	214.5	35.0	207.0	26.0	207.0	6.4	194.0	215.0	19.5
80.0	35.0	214.5	35.0	207.0	24.5	207.0	6.8	194.0	215.0	21.6
90.0	35.0	214.7	35.0	207.0	23.5	207.0	7.0	193.0	214.0	23.6
100.0	35.0	215.0	35.0	207.0	21.5	207.0	7.3	193.0	214.0	25.9

Table 7. Results of the polystyrene extrusion.

	T_{set1}=190°C T_{e1}=193°C		T_{set2}=195°C T_{e2}=200°C		T_{set3}=200°C T_{e3}=204°C		T_{set4}=200°C T_{e4}=207°C			
N (rpm)	P_{i1} (MPa)	T_{i1} (°C)	P_{i2} (MPa)	T_{i2} (°C)	P_{i3} (MPa)	T_{i3} (°C)	P_{exit} (MPa)	T_{exit} (°C)	T_{die} (°C)	$\dot{m}_E$ (kg/h)
70.0	18.8	203.0	31.4	205.0	18.7	210.0	5.8	198.0	225.0	21.8
80.0	18.0	203.0	31.2	205.0	17.8	210.0	5.9	200.0	225.0	24.8
90.0	17.2	204.0	30.7	206.0	17.6	210.0	6.1	198.0	224.0	27.5
100.0	18.7	204.0	29.9	207.0	17.8	209.0	6.4	196.0	226.0	31.2

It must be remarked that the values of pressure in the heating zones 1 and 2 (P_{i1} and P_{i2}, respectively) showed in Table 6 reached the upper limit of output of the pressure sensors used. Therefore, these values cannot be taken as the actual pressure values at these zones.

Tables 6 and 7 show that T_i values were always higher than T_e ones, indicating that the effect of the viscous dissipation was significant in these tests. On the other hand, the values of mass flow rate increase when screw speed increases, in agreement with theoretical knowledge. In the case of the PS extrusion (Table 7) it was possible to measure pressure values also at the two first measurement points (i.e., P_{i1} and P_{i2}). This lower pressure build-up of the PS (in comparison with the PP) is probably due to its solid bed characteristics, primarily, pointing to lower friction coefficients.

3.3. Simulation

For defining materials properties, the data showed in Table 1 (thermal and physical data) and in Table 5 (rheological data) were used. The geometric characteristics of the extruder were defined according to the data showed in Table 2 (screw data) and in Table 3 (positions of the heating zones) were used. For defining extruder operating conditions, it was taken into account the fact that the Flow 2000 uses the barrel temperature as a fixed boundary condition for the melt pool and melt film above the solid bed. For this reason, T_{i1}, T_{i2}, and T_{i3} (Table 6 and Table 7) were used as the temperatures of the heating zones 1, 2, and 3, respectively in the simulations. For setting the temperature at zone 4, it was chosen to use the same value at zone 3, i.e., T_{i3}, since T_{i4} do not represent the actual temperature in fourth heating zone the extruder. The temperature profiles used in the simulations are presented in Table 8.

Table 8. Temperature profiles used in the simulations

Material	N(rpm)	T_1 (°C)	T_2 (°C)	T_3 (°C)	T_4 (°C)
PP	70	214.5	207.0	207.0	207.0
	80	214.5	207.0	207.0	207.0
	90	214.7	207.0	207.0	207.0
	100	215.0	207.0	207.0	207.0
PS	70	203.0	206.0	210.0	210.0
	80	203.0	205.0	210.0	210.0
	90	204.0	206.0	210.0	210.0
	100	204.0	207.0	209.0	209.0

The predictions of Flow 2000 were adjusted to the experimental results through the estimation of the barrel-polymer friction coefficients (f_b). Values for f_b of 0.575 and 0.560 were obtained for PP and PS, respectively. Table 9 shows a comparison between experimental data of mass flow rate ($\dot{m}_E$) and pressure at the exit of the extruder (P_{exitE}) with predicted results from Flow 2000 ($\dot{m}_F$ and P_{exitF}). As can be seen in this table, in the case of PP extrusion simulations, the predictions of the Flow 2000 resulted in higher values of $\dot{m}$ than the experimental data. In addition, the predictions of P_{exit} are in good agreement with experimental ones. On the other hand, for PS simulations, the better agreements between experimental and predicted values were obtained for mass flow rate, primarily, at higher screw speed.

Table 9. Comparison between experimental data of $\dot{m}$ and P_{exit} with predicted results from Flow 2000.

Material	N (rpm)	$\dot{m}_F$ (kg/h)	$\dot{m}_E$ (kg/h)	$\Delta\dot{m}$ (%)	P_{exitF} (MPa)	P_{exitE} (MPa)	ΔP_{exit} (%)
PP	70	20.2	19.5	-3.6	6.7	6.4	-4.1
	80	22.9	21.6	-6.0	6.8	6.8	-1,4
	90	25.5	23.6	-7.9	7.0	7.0	<0.1
	100	28.1	25.9	-8.7	7.1	7.3	2.6
PS	70	22.7	21.8	-4.3	6.3	5.8	-8.5
	80	25.6	24.8	-3.5	6.4	5.9	-8.5
	90	28.5	27.5	-3.4	6.4	6.1	-5.0
	100	31.1	31.2	0.3	6.6	6.4	-3.3

These satisfactory results allowed the use of the simulator for generating extrusion response variables for adjustments of the parameters of the simplified models. Then, a $2^{(20-14)}$ fractional factorial design of experiments (DOE) with resolution IV was applied to define this second set of simulations, using material properties (rheological and thermal) and extruder processing conditions (screw speed and barrel temperature profile) as factors for investigation. This design resulted in 65 simulations (64 plus central point). The lowest level of each factor was defined as 10% lower than the lowest value comparing PP and PS data. Similarly, the highest level of each factor was defined as 10% higher than the highest value comparing PP and PS data. The definition of screw speed and temperature profile was made according to the actual range of processing conditions.

The factors with significant effects in the mass flow rate were η_0, a, λ, ρ_m, T_p, f_b, N, T_1, and T_4, and for pressure at exit of the extruder were λ, T_4, η_0, a , n, and b according to analysis of variance with a confidence level of 95%. Thus, for developing the simplified models for both $\dot{m}$ and P_{exit} calculations, the factors with significant effects were combined generating interactions of second and third (only for P_{exit} model) orders. In fact, the four terms for describing the dependence of the viscosity on shear rate and on temperature were incorporated into rheological models, taking into account the temperature in each barrel heating zone, i.e.:

$$\eta(T_j) = \frac{\eta_0\left(\exp(-b(T_j - T_{ref})\right)}{\left[1 + \left(\lambda\dot{\gamma}\left(\exp(-b(T_j - T_{ref})\right)\right)^a\right]^{\left(\frac{1-n}{a}\right)}}, \text{ j = 1, 2, 3, and 4.} \quad (2)$$

In Eq (2), $\dot{\gamma} = \frac{\pi DN}{H}$, in which D is the diameter of the extruder, N is the screw speed, and H is the height of the metering section (Morton-Jones, 1989).

The combination of the factors resulted in 36 terms in the mass flow rate model, and 41 terms in the pressure at exit of the extruder model. For selecting only the important terms of these equations, SROV method (Shacham and Brauner, 2003) was applied. Basically, this method selects independent variables to enter into the model according to their level of correlation with the dependent variable and they are removed from further consideration when their residual information gets below the noise level. The use of this method resulted in 10 terms in the $\dot{m}$ model, and in 6 terms in the P_{exit} model.

The Eqs. (3) and (4) present the final form for simplified models for calculations of mass flow rate ($\dot{m}_{MS}$) and pressure at exit of the extruder (P_{exitMS}), respectively:

$$\dot{m}_{MS} = 5.4 - 12.5 f_b - 0.00031 \rho_m N - 27236.2 \frac{1}{\eta(T_1)} + 46467.8 f_b \frac{1}{\eta(T_1)} + 5.3 N \frac{1}{\eta(T_2)} + \\ + 0.9 \rho_m \frac{1}{\eta(T_3)} - 24.3 N \frac{1}{\eta(T_4)} + 33.2 T_m \frac{1}{\eta(T_4)} - 364726.1 \frac{1}{\eta(T_2)} \frac{1}{\eta(T_4)} \quad (3)$$

$$P_{exit\,MS} = -3.2 + 0.002 \eta(T_2) + 0.008 \eta(T_4) + 0.09 f_b N - 0.0002 f_b \eta(T_4) - 0.000002 \eta(T_2) \eta(T_4) \quad (4)$$

It can be observed in Eq. (3) and (4) that the terms of viscosity were considered inversely proportional to the mass flow rate, and directly proportional to the pressure at the exit of the extruder.

Figure 2 shows a comparison between predicted results of mass flow rate from the simplified models (*MS*) and from Flow 2000 (*F*).

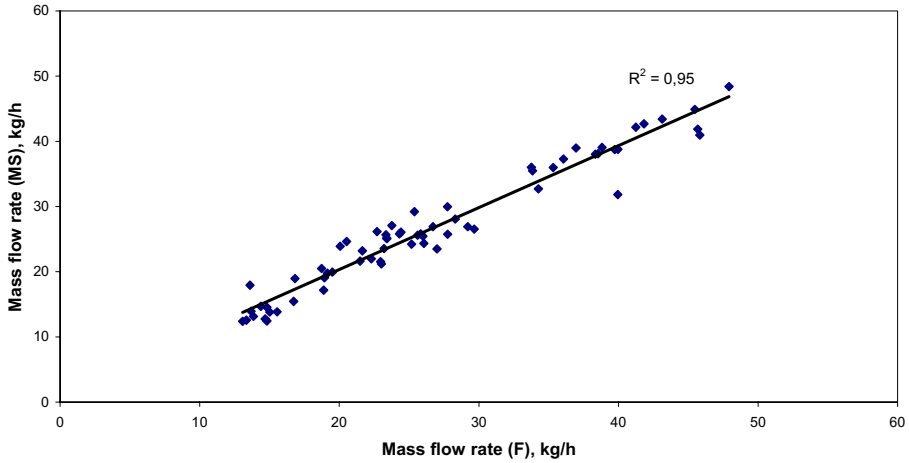

Fig. 2. Comparison between predicted values of the mass flow rate from simplified models and from Flow 2000.

The comparison presented in Fig. 2 indicates that the simplified model is able to represent reasonable well the values of mass flow rate predicted by Flow 2000.

Figure 3 shows a comparison between predicted results of pressure at exit of the extruder from the simplified models (*MS*) and from Flow 2000 (*F*).

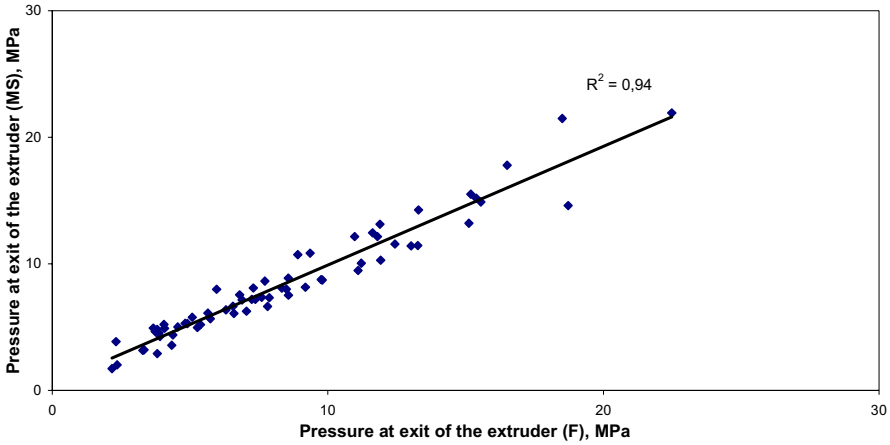

Fig. 3. Comparison between predicted values of the pressure at exit of the extruder from simplified models and from Flow 2000.

As can be seen in Fig. 3, it also was obtained reasonable agreement between the values of the pressure at exit of the extruder predicted by Flow 2000 and by the simplified model.

Table 10 presents a comparison between experimental data of $\dot{m}$ and P_{exit} with predicted results from the simplified models.

Table 10. Comparison between experimental data of $\dot{m}$ and P_{exit} with predicted results from simplified models.

Material	N (rpm)	$\dot{m}_{MS}$ (kg/h)	$\dot{m}_{E}$ (kg/h)	$\Delta\dot{m}$ (%)	P_{exitMS} (MPa)	P_{exitE} (MPa)	ΔP_{exit} (%)
PP	70	21.0	19.5	-7.4	6.0	6.4	6.7
	80	23.5	21.6	-8.7	6.1	6.8	9.6
	90	25.9	23.6	-9.5	6.3	7.0	10.0
	100	28.2	25.9	-9.1	6.5	7.3	10.5
PS	70	24.4	21.8	-12.0	6.3	5.8	-9.0
	80	27.5	24.8	-10.9	6.4	5.9	-8.7
	90	30.5	27.5	-10.7	6.5	6.1	-6.2
	100	33.3	31.2	-6.6	6.8	6.4	-6.4

In Table 10, it can be seen that the percentage difference between the experimental and predicted values from simplified model of $\dot{m}$ and P_{exit} are in range of 10% for both PP and PS analysis. This is the same range obtained comparing the experimental data with predicted results from Flow 2000, i.e., the power of prediction capability for mass flow rate and pressure at exit of the extruder of both methods are equivalent.

4. Conclusion

Simplified models for the prediction of mass flow rate ($\dot{m}$) and pressure (P_{exit}) at the exit of extruders as functions of material properties and extruder operating conditions, using experimental data and predictions of a commercial extrusion simulator, were presented. Good agreements between experimental and predicted values

of $\dot{m}$ and P_{exit} were achieved when the simplified models were applied. Thus, these simplified models are more economically attractive than computational packages commercially available and are more accurate than conventional analytical equations, which do not take into account solids conveying and non-Newtonian behavior of the polymers. For instance, these models can be used for fast decision making related to the extruder operating conditions during resin change.

Complementary study will be made in order to assembly the flow behavior of the polymer into the extruder and into the die, allowing the development of more versatile models for extrusion analysis.

References

Cunha, A. L. (2000). Modelling and Optimisation of Single-Screw Extrusion. *PhD Thesis*, Guimarães.

Flow 2000. (2002). *Flow 2000, User Guide*, CD-ROM, v.5.2.

Han, C. D., Lee, K. Y. Wheeler, N. C. (1996). Plasticating Single-Screw Extrusion of Amorphous Polymers: Development of a Mathematical Model and Comparison with Experiment, *Polym. Eng. and Sci., 36, 1360*.

MC Base (2002), *CAMPUS Data base*, CD-ROM, v. 4.5.

Menges, G.; Osswald T. A. (1996). Materials Science of Polymers for Engineers, *(eletronic version)*.

Moore, E. R. (1989). The Dow Chemical Company, Reprint of the Encyclopedia of Polymer and Engineering, 2ª ed., John Wiley & Sons, New York.

Morton-Jones, D.H. (1989). Polymer Processing, Chapman & Hall, London.

Rauwendaal, C. (1986). Polymer Extrusion, 3ª ed., Carl Hanser Verlag, Munich.

Shacham, M., Brauner, N. (2003). The SROV Program for Data Analysis and Regression Model. *Comput. Chem. Eng.*, *27*, 701.

Tadmor, Z., Klein, I. (1970). Engineering Principles of Plasticating Extrusion, Van Nostrand Reinhold, New York.

Wolf, C. R., Grave, E. (2002), A study of Parameters Related to Analysis of Transition Temperatures and Enthalpies of Polypropylene by Differential Scanning Calorimetry (DSC). *J. of Chem*., 10, 73.

Zhang, X., Hendro, W., Fujii, M., Tomimura, T., Imaishi, N. (2002). Measurements of the Thermal Conductivity and Thermal Diffusivity of Polymer Melts with Short-Hot-Wire Method. *Int. J. Thermophysics*, 23, 1077.

Acknowledgments

The authors wish to acknowledge INNOVA S/A and CAPES for providing the financial support to carry out this work. Special thanks to the R&D group of Petroquimica Cuyo and Miguel Sforza (Petrobras Energía) for assistance in the acquisition of the experimental data.